



Published in final edited form as:

Hepatology. 2019 June ; 69(6): 2518–2532. doi:10.1002/hep.30528.

## An Efficient Combination Immunotherapy for Primary Liver Cancer by Harmonized Activation of Innate and Adaptive Immunity

Liang Wen<sup>1,2</sup>, Bing Xin<sup>1</sup>, Panyisha Wu<sup>1,2</sup>, Chia-Hao Lin<sup>3</sup>, Chuanhui Peng<sup>1,4</sup>, Gaowei Wang<sup>1</sup>, Jin Lee<sup>1</sup>, Li-Fan Lu<sup>3</sup>, and Gen-Sheng Feng<sup>1</sup>

<sup>1</sup>Department of Pathology, Division of Biological Sciences, and Moores Cancer Center, University of California at San Diego, La Jolla, CA 92093, USA.

<sup>2</sup>Department of General Surgery, Second Affiliated Hospital of Zhejiang University, Hangzhou, 310000, P.R. China.

<sup>3</sup>Division of Biological Sciences, Center for Microbiome Innovation and Moores Cancer Center, University of California at San Diego, La Jolla, CA 92093, USA.

<sup>4</sup>Department of Surgery, First Affiliated Hospital of Zhejiang University School of Medicine, Hangzhou, 310003, P.R. China

### Abstract

Immunotherapy with checkpoint inhibitors for liver cancer, while active in many clinical trials worldwide, may have uncertain outcomes due to the unique immunotolerant microenvironment of the liver. In previous experiments, we unexpectedly identified a robust liver tumor-preventive effect of a synthetic double-stranded RNA (dsRNA) polyinosinic-polycytidylic acid (polyIC) in mice. Herein we further demonstrate that polyIC given at the pre-cancer stage effectively prevented liver tumorigenesis by activating NK cells, macrophages and some T cell subsets; no inhibitory effect was observed on tumor progression if injected after tumor initiation.

Nevertheless, polyIC administration potently induced PD-L1 expression in liver sinusoid endothelial cells, which prompted us to test a combined treatment of polyIC and PD-L1 antibody (Ab). Although injecting PD-L1 Ab alone did not show any therapeutic effect, injection of polyIC sensitized hepatic response to PD-L1 blockade. Combination of polyIC and PD-L1 Ab resulted in sustained accumulation of active CD8 cytotoxic T cells and robust liver tumor suppression, and conferred survival advantage in mice. These preclinical data in animal models suggest that, despite the low efficacy of PD-L1/PD-1 blockade alone, careful design of mechanism-based combinatorial immunotherapeutic protocols may shift the paradigm in liver cancer treatment, by coordinating maximal activation of multiple innate and adaptive immune functions. *Conclusion:* We provide proofs of principle for development of an efficient prevention strategy of liver tumorigenesis and a powerful combination immunotherapy for primary liver cancer.

## Keywords

Liver cancer prevention; combination immunotherapy; PD-L1/PD-1 blockade; synthetic dsRNA

---

## INTRODUCTION

Primary liver cancer, with the majority being hepatocellular carcinoma (HCC), is now the second leading cause of cancer mortality and the fifth most common cancer worldwide.<sup>(1–3)</sup> HCC is a chemotherapy-resistant tumor with limited treatment options of surgical resection, liver transplantation and local ablation at the early stages. Sorafenib, a multi-kinase inhibitor, remains a first-line systemic drug for advanced HCC despite its poor outcomes.<sup>(4, 5)</sup> Similar low therapeutic benefits were reported for regorafenib, lenvatinib, and cabozantinib.<sup>(6–8)</sup> Over 100 clinical trials that tested other compounds or approaches have failed to show significant therapeutic effect on HCC patients.<sup>(9)</sup>

Immunotherapy by blocking inhibitory pathways in T lymphocytes, such as the PD-L1/PD-1 axis, is being widely tested in various solid tumors.<sup>(10–12)</sup> This emerging therapeutic approach is already in clinical trials for advanced HCC in multi-centers around the globe.<sup>(13, 14)</sup> Two latest reports on open-label, non-randomized, phase 1/2 trials with pembrolizumab or nivolumab indicated manageable safety in advanced HCC patients with or without prior sorafenib treatment, albeit with very limited therapeutic benefit observed so far.<sup>(15, 16)</sup> The outcome of immunotherapy for liver cancer is compounded by the unique immunotolerant microenvironment in the liver.<sup>(17, 18)</sup> A variety of clinical trials are ongoing to evaluate various combinations of immune checkpoint inhibitors or with other drugs, without clear justification or support by preclinical data in animal models.<sup>(19)</sup>

In previous study, we identified unexpectedly a potent liver tumor-inhibitory role of a synthetic double stranded RNA (dsRNA), polyinosinic-polycytidylic acid (polyIC), in experiments originally designed to decipher the anti-oncogenic role of tyrosine phosphatase Shp2 in the liver.<sup>(20)</sup> Injection of polyIC at the pre-cancer stages effectively prevented liver tumor initiation in mouse models for HCCs induced by chemical carcinogen or Pten loss and associated non-alcoholic steatohepatitis (NASH). In this study with mouse HCC models driven by transfection of oncogenes, we confirmed the previous observation on a robust inhibitory effect of the dsRNA in liver cancer initiation but not on tumor progression. However, based on the data of a potent induction of CD274 (PD-L1) expression by polyIC in the liver, we tested a combination immunotherapy of polyIC and anti-PD-L1 antibody (Ab). Herein we report for the first time that combined treatment of the two reagents effectively suppressed HCC progression in animal models, although neither showed any therapeutic effect alone. These preclinical data may be instrumental for design of combinatorial therapy for HCC, using polyIC and PD-L1 Ab or other similar reagents that can boost both innate and adaptive immune activities.

## MATERIALS AND METHODS

### Mice and tumor models.

All animals in this study were wild-type C57BL/6J mice from Jackson Laboratory, and male mice at age of 7–9 weeks were used for the experiments. The animal protocols (S09108) were approved by the Institutional Animal Care and Use Committee (IACUC) of the University of California San Diego, following National Institutes of Health guidelines. Mouse liver tumors were induced by hydrodynamic tail vein injection (HTVi) of oncogenes together with the sleeping beauty transposase, as described previously.<sup>(21–23)</sup> The plasmids (PT3-EF1a-C-Myc; PT/Caggs-NRas-V12; PT3-EF1a-c-Met; pT3-EF1a-N90- $\beta$ -catenin; pCMV-SB11) were gifts from Dr. X Chen at UCSF. The GFP-expressing plasmid (PT3-EF1a-EGFP) was constructed by cloning. All plasmid DNAs were diluted in PBS and injected at 0.1 ml/g body weight through tail vein in 5–7 seconds.

### Drug administration and cell depletion assays.

PolyIC (GE Healthcare) was injected intraperitoneally (i.p.) at 4 mg/kg every other day for five doses at the indicated dates. Anti-mouse PD-L1 Ab (BE0101, Bioxcell) was i.p. injected at 200  $\mu$ g (or 200  $\mu$ g of rat IgG2b, BE0090, Bioxcell, as isotype control) every other day for three doses as indicated. For NK cell depletion, mice were i.p. injected with 600  $\mu$ g of NK1.1 Ab (BE0036, Bioxcell), or 600  $\mu$ g of mouse IgG2a (BE0085, Bioxcell) as isotype control one time at the indicated date. Macrophages were depleted by i.p. injection of 200  $\mu$ L of clodronate liposome (C09T0317, [www.liposome.com](http://www.liposome.com)), or 200  $\mu$ L of PBS control liposome (P08T0317, [www.liposome.com](http://www.liposome.com)) one time as indicated. CD8 T cells were depleted by i.p. injection of 200  $\mu$ g of anti-mouse CD8 $\alpha$  (BE0061, Bioxcell), or 200  $\mu$ g of rat IgG2b (BE0090, Bioxcell) as isotype control three or five times as indicated.

### RNA sequencing and bioinformatic data analysis.

Immune cells were isolated from mouse liver and total RNAs were extracted using RNeasy Microarray Tissue Mini Kit (QIAGEN #73304). cDNA libraries were prepared using Illumina TruSeq Stranded mRNA Library Prep Kit (RS-122–2101, Illumina). RNA-sequencing (RNA-seq) was performed using Illumina HiSeq 4000 at the IGM Genomics Center, UCSD. RNA-seq generated raw data were aligned to the GRCm38 mouse reference genome using Star program (2.3.0). Gene differential expression analysis was performed using Cuffdiff to obtain the gene expression levels in each sample. The significant differences in gene expression were based on q values ( $<0.05$ ) and fold change ( $>2$ ). Gene set enrichment analysis (GSEA) was performed for pathway analysis online ([software.broadinstitute.org/gsea](http://software.broadinstitute.org/gsea)). Heatmaps were generated with the heatmap package using R program.

### Statistical analysis.

Statistical analysis was done using GraphPad Prism 6.01 or 7.0a. Values were presented as means  $\pm$  SD. Statistical significance between means was performed using Student's T-Test. qPCR data analysis was done using Mann-Whitney U test. Survival curves were plotted by

Kaplan-Meier analysis and compared using the log-rank test. P value <0.05 was considered significant (\*p < 0.05, \*\*p < 0.01).

## RESULTS

### PolyIC inhibits tumor initiation but not progression in the liver

In previous experiments aimed at dissecting hepatocyte and Kupffer cell communication during liver tumorigenesis, we found that polyIC, an inducer of the *Mx1-Cre* gene deletion system, had a potent tumor-inhibitory effect independent of the inducible gene ablation.<sup>(20)</sup> To determine this intriguing role and mechanism, we expanded the observation to other mouse HCC models that are driven by oncogene transfection via HTVi.<sup>(21)</sup> Using this approach, we injected two plasmids (Ras/Myc) that express human N-Ras and human c-Myc, together with a *sleeping beauty* transposase construct (Supporting Fig. S1A). Mice were sacrificed for phenotypic analysis at 2, 4, 6 weeks. Liver tumor nodules were visible as early as 4 weeks and progressed rapidly, as examined macroscopically and by H&E staining of liver sections (Supporting Fig. S1B), statistical analysis of liver weight/body weight (LW/BW) ratios, maximal diameters and numbers of tumor nodules, as well as increased spleen/body weight ratios (Supporting Fig. S1C–F).

We evaluated the tumor-suppressing activity of polyIC injected before or after tumor induction by Ras/Myc. The synthetic dsRNA was injected i.p. every other day for a total of 5 doses and the tumor burdens were examined 4 and 6 weeks after oncogene transfection (Fig. 1A). polyIC given before tumor initiation by oncogenes (pre-polyIC) significantly suppressed tumor formation, as determined by macroscopic and histological examination, LW/BW ratios, maximal sizes and numbers of tumor nodules (Fig. 1B–E). However, polyIC administration starting 2 weeks after oncogene transfection (post-polyIC) did not have significant inhibition on tumor burdens examined by these criteria (Fig. 1B–E). Further, the LW/BW ratios even increased significantly in the post-polyIC group compared to the control, likely due to enhanced inflammation. These results suggest that polyIC given at the pre-cancer stage can efficiently prevent tumor initiation driven by the oncogenes, consistent to previous data on HCC induced by diethylnitrosamine (DEN), or HCC and ICC (intrahepatic cholangiocarcinoma) driven by Pten deletion and NASH.<sup>(20)</sup> Notably, polyIC alone did not have therapeutic effect if given after tumor initiation as shown here and in previous studies.<sup>(20)</sup>

### Activation of innate immunity is required for the tumor-preventive effect of polyIC

We investigated if pre-polyIC treatment had influenced genomic integration of the exogenous oncogenic cDNAs into hepatocytes, as delivered by the HTVi approach.<sup>(21)</sup> A GFP-expressing plasmid was injected into mice via HTVi with or without pre-treatment of polyIC (Supporting Fig. S2A). Genomic DNA was extracted from liver lysates 7 days later for quantitative PCR analysis. Similar levels of the GFP cDNA were detected between the two groups (Supporting Fig. S2B), suggesting polyIC pre-treatment does not affect plasmid DNA transfection and integration into the hepatocyte genome.

Next, we interrogated the effects of polyIC on various immune cell subsets under different conditions (Fig. 2A). By comparing the WT livers with or without polyIC treatment, we determined an impact of polyIC itself, without liver damage caused by the HTVi procedure. Comparing the polyIC effects in livers that received GFP or Ras/Myc oncogenes, we also evaluated the influence of tumor development on polyIC-induced immune alterations. As shown in Fig. 2B, polyIC treatment induced significant population increase of macrophages and NK cells, with a modest effect on myeloid-derived suppressor cells (MDSC) and no significant impact on dendritic cells (DC) in all three polyIC-treated groups, relative to the WT control. Furthermore, polyIC injection increased the numbers of CD8 T cells and regulatory T cell (Treg), while the CD4 T cells and B cell populations were unchanged or modestly decreased (Fig. 2B). The changes in various cell subsets were quite similar among the three polyIC-treated groups, relative to the WT control (Fig. 2B), suggesting that polyIC modulation of immunity is independent of the hydrodynamic injection.

As the previous data suggested possible involvement of NK cells and macrophages in polyIC-mediated clearance of tumor-initiating cells (TICs),<sup>(20)</sup> we sought to determine if these cell subsets were responsible for polyIC's inhibition of HCC. Anti-NK1.1 antibody, clodronate liposome, or anti-CD8 antibody was injected to deplete or block NK cells, macrophages or CD8 T cells (Supporting Fig. S3A). At 2 days after last polyIC injection, liver NPC cells were isolated for FACS analysis to evaluate the depletion efficiency (Supporting Fig. S3A). The numbers of macrophages, NK and CD8 T cells decreased markedly after injection of the corresponding reagents, without or with polyIC injection (Supporting Fig. S3). We then asked if depletion of these cell subsets had any impact on tumorigenesis, by examining the tumor loads 6 weeks after Ras/Myc transfection (Supporting Fig. S4A). In mice without pre-polyIC treatment, depletion of these cell subsets did not significantly change tumor burden (Supporting Fig. S4B). Therefore, the basal activities of NK cells, macrophages or CD8 T cells in the liver had little effect on liver tumorigenesis. However, depletion of NK cells or macrophages abrogated the tumor-inhibitory effect of pre-polyIC treatment, with no effect of CD8 T cell depletion observed (Fig. 2C). These data indicate that polyIC inhibition of HCC initiation is dependent on activation of NK cells and macrophages, but not CD8 T lymphocytes.

### **PolyIC upregulates PD-L1 expression in liver sinusoid endothelial cells (LSEC)**

Previous RNA-seq analysis detected significant increase of CD274 (PD-L1) expression in polyIC-treated livers.<sup>(20)</sup> Consistently, immunoblotting detected high levels of PD-L1 protein contents in livers treated with polyIC, regardless of oncogene transfection (Fig. 3A). We then examined PD-L1 expression patterns in the liver, and found that the PD-L1 signal was markedly elevated in LSECs, noted by co-localization with the endothelial marker VE-cadherin (Fig. 3B), with no increase of PD-L1 expression in tumor areas in Ras/Myc-transfected livers. Flow cytometry showed very similar results (Fig. 3C), and the mean fluorescence intensity (MFI) of PD-L1 expression was markedly increased in LSECs of all polyIC-treated groups, relative to the modest increase in non-LSECs (Fig. 3D). Consistently, higher PD-L1 induction by polyIC was detected in LSECs than isolated DCs and macrophages (Supporting Fig. S5), a bit different from other data showing polyIC upregulation of PD-L1 expression in DCs or epithelial cells.<sup>(24–26)</sup>

To define a direct role of polyIC in PD-L1 induction, we cultured LSECs isolated from WT mouse livers. The PD-L1 mRNA level was significantly elevated in LSECs after polyIC treatment for 2 days (Fig. 3E), suggesting that PD-L1 induction in LSECs by polyIC in the liver was independent of oncogene transfection or tumor development. We also assessed polyIC impact on PD-1 expression in infiltrated lymphocytes including CD4, CD8 T cells and B cells. Following polyIC treatment, PD-1-positive cell ratios were higher in CD4 and CD8 T cells, but not in B cells, than the controls (Fig. 3F). Thus, polyIC treatment likely induced T cell dysfunction at least in part by promoting PD-L1/PD-1 signaling in the liver.

### Combination of polyIC and PD-L1 blockade suppresses HCC progression

Given that PD-L1 expression is required for the anti-tumor effect of PD-1/PD-L1 blockade,<sup>(27)</sup> the data on polyIC induction of PD-L1 prompted us to explore an immunotherapeutic strategy for HCC by combined treatment of polyIC and PD-L1 Ab. The Ras/Myc-transfected mice were treated with polyIC, PD-L1 Ab or combination of polyIC and PD-L1 Ab (Combo), starting 2 weeks after oncogene transfection, with tumor burdens examined at 6 weeks (Fig. 4A). Injection of either polyIC or PD-L1 Ab failed to reduce the tumor loads, showing similar liver sizes and numbers of tumor nodules as the control (Fig. 4B). However, combination of polyIC and PD-L1 Ab significantly suppressed tumor progression, evaluated by macroscopic view and H&E staining or by the LW/BW ratios, sizes and numbers of tumor nodules (Fig. 4B–C). H&E staining showed necroptosis, apoptosis and lymphocyte infiltrations in tumor tissues, and immunostaining and immunoblotting also detected higher levels of cleaved caspase 3 and pRIPK3 following the combined treatment (Supporting Fig. S6A–B).

We detected no significant changes in Ki67<sup>+</sup> cell ratios in tumor areas in the polyIC or anti-PD-L1 group, compared to the control. However, the combined treatment significantly decreased the Ki67<sup>+</sup> ratios in the tumor areas (Fig. 4D). Mouse survival analysis showed the median survival time 58.0±9.3, 77.5±11.8, 64.5±14.2 and 91±27.0 days for the control, polyIC, anti-PD-L1 and the combination groups (Fig. 4E). Overall, the median survival time was similar between the anti-PD-L1 and control groups, and the combo group exhibited most significant extension of survival, with 2 mice still alive at the end point of observation (18 weeks after oncogene injection). We also explored a therapeutic effect of the combination at later stages of tumor progression, with the treatment starting at 3 or 4 weeks after Ras/Myc transfection. Again, co-injection of polyIC and PD-L1 Ab significantly decreased tumor burdens, compared to the control (Fig. 4F).

We tested the combination therapy in another HCC model by transfection of constructs (MET/CAT) expressing human c-MET and a truncated  $\beta$ -catenin mutant,<sup>(23, 28)</sup> two oncogenes that are frequently detected in human HCC patients.<sup>(29)</sup> Based on the pathogenic process in this model, we started the treatment 6 weeks after MET/CAT transfection, and examined the tumor loads at 8 weeks (Supporting Fig. S7A). Macroscopic view showed that neither polyIC nor PD-L1 Ab inhibited HCC development, while no tumor nodules were visible in the combination group. H&E staining also showed similar results. More infiltrated mesenchymal cells were in the liver treated with the combination (Supporting Fig. S7B). Statistical analysis showed modest decrease of tumor burdens following treatment of polyIC

or anti-PD-L1 alone, with the most remarkable effect observed in the combination group (Supporting Fig. S7C). Therefore, a combination of polyIC and PD-L1 Ab exhibited potent inhibition on HCCs of different etiologies.

### Sensitization of PD-L1 blockade by polyIC boosts anti-tumor immunity in the liver

We dissected the underlying mechanisms for the robust tumor-inhibitory effect of the combined treatment. Ras/Myc-transfected mice treated with polyIC, PD-L1 Ab or the combo as in Fig. 4A were sacrificed 2 days after the last polyIC injection. Immunostaining demonstrated significantly increased infiltration of CD45<sup>+</sup> cells into livers treated with polyIC or anti-PD-L1, but the combo caused even more infiltration of CD45<sup>+</sup> cells into the liver (Fig. 5A, top). We also isolated and counted the CD45<sup>+</sup> cells from WT livers without oncogene transfection. The numbers of total immune cells ( $4.51 \pm 0.51 \times 10^6$ ) in untreated Ras/Myc-transfected livers were similar to the WT ( $5.11 \pm 0.66 \times 10^6$ ). polyIC or PD-L1 Ab treatment significantly increased the number of immune cells in livers to  $11.92 \pm 1.52 \times 10^6$  and  $12.52 \pm 2.80 \times 10^6$ , respectively. However, the immune cell numbers were markedly increased to  $27.27 \pm 3.05 \times 10^6$  in livers treated with the combination (Fig. 5A, down).

We performed more detailed FACS analysis of several innate and adaptive immune cell subsets in the liver. The relative cell numbers were calculated as ratios in the total numbers of NPCs, except the Treg cells, which were calculated as a ratio to the total CD4 T cells. Flow cytometry was performed on innate immune cells, including macrophages (CD11b<sup>+</sup> F4/80<sup>+</sup>), NK cells (CD4-NK1.1<sup>+</sup>), DCs (MHC II<sup>+</sup> CD11c<sup>+</sup>) and MDSCs (CD11b<sup>+</sup> Gr1<sup>+</sup>) (Supporting Fig. S8A). Compared to the control, polyIC injection significantly increased macrophages and NK cells, which were not influenced by PD-L1 Ab treatment; the combination also increased macrophages and NK cells significantly. There was no significant difference of DC numbers between these groups. Treatment of polyIC alone or the combination had similar effects in decreasing MDSC (Fig. 5B). We then analyzed adaptive immune cell subsets, including conventional CD4 T cell (CD4<sup>+</sup>Foxp3<sup>-</sup>), CD8 cytotoxic T cell (CD4<sup>-</sup>CD8<sup>+</sup>), Treg (CD4<sup>+</sup>Foxp3<sup>+</sup>) and B cell (CD4<sup>-</sup>CD45R<sup>+</sup>), by flow cytometry (Supporting Fig. S8B). Treatment of polyIC alone or in combination with PD-L1 Ab caused similar decrease of CD4 lymphocytes, while PD-L1 Ab did not impact the CD4 cell ratio. Interestingly, the number of CD8 T cells was modestly increased in polyIC-treated liver, but was dramatically elevated to  $46.85 \pm 2.84\%$  of all NPCs in livers treated with the combination. The ratio of Treg cells in CD4 T cell pool was significantly increased by PD-L1 Ab, but increased even more in livers treated with polyIC or the combination (Fig. 5C).

We performed RNA-seq analysis of isolated CD45<sup>+</sup> immune cells infiltrated into the liver. The differentially expressed genes, including up- and down-regulated, were identified by cut-off of 2-fold with q-value of <0.05. The list in Supporting Fig. S9A showed a total of 1654 differentially expressed genes specifically in the combination group. Gene set enrichment analysis (GSEA) of these 1654 genes demonstrated that the immune cells in the combination group were particularly associated with adaptive and innate immune system and the antigen processing/presentation, pointing to an enhanced anti-tumor immunity (Supporting Fig. S9B). We also listed the key genes involved in interferon- $\gamma$  (IFN $\gamma$ ) signaling pathway (Supporting Fig. S9C, top), which was regarded as sign of activated anti-

tumor immunity.<sup>(30)</sup> A heatmap showed that the combination treatment maximized IFN $\gamma$  signaling in hepatic immune cells. Also upregulated most profoundly in the combo group were some key genes, perforin (Prf1), granzyme B (Gzmb), IFN $\gamma$  (Ifng), indicators of anti-tumor cytotoxic function (Supporting Fig. S9C, bottom). The RNA-seq data also showed polyIC-induced expression of a number of chemokines and chemokine receptors, which was confirmed by qRT-PCR analysis (Supporting Fig. S9D). All these changes collectively contributed to CD8 T cell accumulation in the liver.

### The effect of combination therapy is cytotoxic T cell-dependent

Evidently, the combination of polyIC and PD-L1 Ab caused dramatic accumulation of CD8 T cells and activation of their cytotoxic activities. We further examined changes of CD8 T cells immediately after various treatments as shown in Fig. 5A. Flow cytometry was performed to analyze the proliferation (Ki67<sup>+</sup>), activation (CD44<sup>+</sup> CD62L<sup>-</sup>) and cytotoxic function (Granzyme B<sup>+</sup>) of CD8 T cells (Supporting Fig. S7C). Interestingly, PD-L1 Ab treatment only slightly enhanced the activation of CD8 T cells but failed to affect their proliferation and cytotoxic function. polyIC treatment enhanced proliferation, activation and cytotoxic function of CD8 T cells, and its combination with PD-L1 Ab further boosted proliferation and activation of CD8 T cells (Fig. 6A), contributing to tumor suppression. We then asked if these changes of CD8 T cells detected in the early phase were maintained in the late phase. Immunostaining of liver sections collected at 6 weeks (Fig. 4A) showed that the numbers of CD8 T cells in both tumor and non-tumor areas were much higher in the combo group (Fig. 6B–C). However, the accumulation of CD4 T cells, B cells, macrophages and neutrophils was similar among the four groups at the late stage (Supporting Fig. S10A–D). Thus, the combination treatment induced a sustained CD8 T cell accumulation in the liver. Finally, to determine a functional requirement of CD8 T cells in the combination therapy, we injected CD8 Ab to block CD8 T cell function (Fig. 6D). Although CD8 Ab did not affect HCC development in this model, CD8 blockade impaired the tumor-inhibitory effect of the combined treatment (Fig. 6E), indicating a critical role of cytotoxic CD8 T cells in mediating the anti-tumor immunity of combined treatment of polyIC and PD-L1 Ab.

## DISCUSSION

This and a previous study<sup>(20)</sup> clearly demonstrate a tumor-preventive effect of the synthetic dsRNA polyIC in several mouse models for liver tumors induced by transfection of oncogenes, chemical carcinogen DEN, and Pten deficiency and associated NASH.<sup>(20)</sup> Notably, polyIC injection enhanced accumulation and activation of innate immune cells in the liver, especially NK cells and macrophages, independent of tumor development. Coordinated activation of these innate immune cells leads to elimination of transforming hepatocytes or TICs, resulting in prevention of tumor initiation.

As a putative cancer vaccine adjuvant, polyIC was shown to induce secretion of various pro-inflammatory cytokines by different immune cell types and tumor cells.<sup>(31)</sup> Previous studies suggested that polyIC could prime and activate DC and stimulates its cross-priming.<sup>(32, 33)</sup> We detected only a minor effect of polyIC on DCs in the liver; however, polyIC induced reprogramming of macrophage polarization towards an M1 phenotype and NK cell



activation in the liver.<sup>(20)</sup> It is likely that polyIC caused coordinated activation of multiple innate immune functions that resulted in cell senescence and clearance of TICs in the liver.<sup>(20)</sup> Consistently, polyIC was shown to activate NK cells and upregulate their cytolytic activity.<sup>(34, 35)</sup> The current study confirmed accumulation of NK cells and macrophages in polyIC-treated livers, and also demonstrated that depletion of the two cell subsets abrogated the tumor-preventive effect of polyIC. Therefore, we believe that boosting innate immunity by pharmaceuticals or other means may be a powerful strategy to prevent tumorigenesis in a huge group of subjects with chronic liver diseases who are at high risk for HCC.

Despite a robust tumor-preventive role of polyIC injected at pre-cancer stages, we showed consistently that administration of polyIC during tumor progression did not have significant therapeutic effect. Further, we found that injection of polyIC alone may even aggravate liver tumorigenesis that is highly associated with inflammation (data not shown). The anti-tumor effect of polyIC has been explored for several decades, and it was on the National Cancer Institute's list of immunotherapeutic agents.<sup>(36)</sup> However, data presented here raise a caution on any clinical trial for liver cancer using this synthetic reagent alone.

We asked why polyIC was insufficient to suppress tumor progression. In addition to its activation of innate immunity, polyIC also modulated the adaptive immune functions, with modest accumulation of CD8 T cells in the liver. In spite of the decreased accumulation of MDSC, polyIC also elevated the ratio of Treg cells. Although CD8 T cell infiltration was enhanced, the dsRNA induced remarkably elevated PD-1 expression in CD4 and CD8 T cells. Together, these multiple factors likely compromised its anti-tumor effect. Consistent with the previous RNA-seq analysis detecting increased CD274 (PD-L1) expression in polyIC-treated liver,<sup>(20)</sup> immunoblot analysis showed substantial increase of PD-L1 in livers treated with polyIC, regardless of the background (Fig. 3A). Therefore, polyIC, while activating innate immunity, also promotes PD-L1/PD-1 signaling in the liver, resulting in T cell exhaustion.

However, this data also inspired us to test an idea of combined treatment of polyIC with PD-L1 Ab. Indeed, data presented here indicate high efficacy of this combination therapy. We observed robust suppression of tumor progression in several mouse models driven by oncogenes frequently detected in human HCC patients, and the effect was observed when injecting the two reagents at early or advanced stages of tumor progression. Of note, polyIC induced PD-L1 expression mainly in LSECs in the liver. LSECs constitute a special structural component and function as the first immune barrier against gut microbiota and a platform for nutrient exchange through endocytosis. More recently, LSECs have been recognized as a special type of antigen-presenting cell (APC) in the liver, capable of cross-presenting soluble exogenous antigens to CD8 T cells, leading to its tolerance.<sup>(37)</sup> It was also shown that circulating carcinoembryonic antigen was preferentially taken up and cross-presented by LSECs to promote CD8 T cell tolerance.<sup>(38)</sup> Clearly, the anti-tumor immunity in the liver can be boosted by coordinated infiltration and activation of cytotoxic T cells through combined treatment of polyIC and PD-L1 Ab.

Encouraged by beneficial responses in some patients with solid tumors, checkpoint inhibitors are already in numerous clinical trials for HCC worldwide, although the outcomes

are uncertain. One serious concern is the low or no response of HCC due to the unusual immunotolerant liver microenvironment. Indeed, we failed to observe any tumor-inhibitory effect of PD-L1 Ab alone in mouse HCC models in this study. Consistently, no significant PD-L1 upregulation was detected in tumor cells, surrounding hepatocytes or NPCs during HCC progression, which predict low response of HCCs to PD-L1 blockade. However, we believe that this issue can be remedied by concerted activation of both innate and acquired immune functions in the liver. As polyIC induction of PD-L1 in LSECs was independent of tumor formation, this therapeutic strategy can be applied to HCCs of various etiologies. It was reported that combination of polyIC and PD-L1 Ab showed inhibitory effect on tumors grown subcutaneously from inoculated melanoma, lung and colon cancer cell lines.<sup>(39)</sup> However, either of these two reagents alone also significantly inhibited subcutaneous tumor growth, apparently due to lack of authentic tumor microenvironment in that artificial system. Herein we report for the first time that only the combination of polyIC and PD-L1 Ab has therapeutic effect on primary liver cancer in mouse models.

The combined treatment showed high therapeutic efficacy at early and late stages of HCC progression, with complete tumor remission and tumor-free survival observed in a few mice. Nevertheless, these data provide only a proof of principle for a new combination therapy. We believe that optimization of the procedures and dosages, and use of other similar but more effective reagents, will hopefully generate even better outcomes in HCC therapy.

## Supplementary Material

Refer to Web version on PubMed Central for supplementary material.

## ACKNOWLEDGEMENT

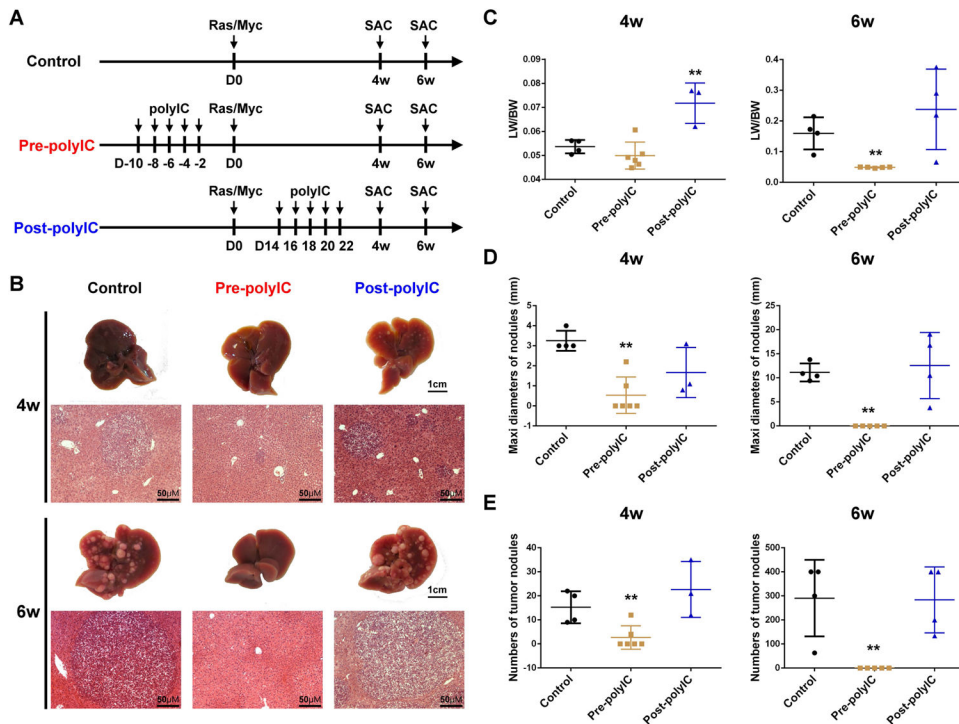
We wish to thank the Feng lab fellows for helpful discussion and critical reading of the manuscript, and Dr. X Chen (UCSF) for the oncogene constructs. This project was supported by NIHR01CA176012 and R01CA1188506 (to G.S.F.) and R01AI108651 and R56AI127751 (to L.F.L.).

## REFERENCES

1. Ferlay J, Soerjomataram I, Dikshit R, Eser S, Mathers C, Rebelo M, Parkin DM, et al. Cancer incidence and mortality worldwide: sources, methods and major patterns in GLOBOCAN 2012. *Int J Cancer* 2015;136:E359–386. [PubMed: 25220842]
2. Llovet JM, Zucman-Rossi J, Pikarsky E, Sangro B, Schwartz M, Sherman M, Gores G. Hepatocellular carcinoma. *Nat Rev Dis Primers* 2016;2:16018. [PubMed: 27158749]
3. Ryerson AB, Ehemann CR, Altekruse SF, Ward JW, Jemal A, Sherman RL, Henley SJ, et al. Annual Report to the Nation on the Status of Cancer, 1975–2012, featuring the increasing incidence of liver cancer. *Cancer* 2016;122:1312–1337. [PubMed: 26959385]
4. Llovet JM, Ricci S, Mazzaferro V, Hilgard P, Gane E, Blanc JF, de Oliveira AC, et al. Sorafenib in advanced hepatocellular carcinoma. *N Engl J Med* 2008;359:378–390. [PubMed: 18650514]
5. European Association For The Study Of The L, European Organisation For R, Treatment Of C. EASL-EORTC clinical practice guidelines: management of hepatocellular carcinoma. *J Hepatol* 2012;56:908–943. [PubMed: 22424438]
6. Bruix J, Qin S, Merle P, Granito A, Huang YH, Bodoky G, Pracht M, et al. Regorafenib for patients with hepatocellular carcinoma who progressed on sorafenib treatment (RESORCE): a randomised, double-blind, placebo-controlled, phase 3 trial. *Lancet* 2017;389:56–66. [PubMed: 27932229]

7. Kudo M, Finn RS, Qin S, Han KH, Ikeda K, Piscaglia F, Baron A, et al. Lenvatinib versus sorafenib in first-line treatment of patients with unresectable hepatocellular carcinoma: a randomised phase 3 non-inferiority trial. *Lancet* 2018;391:1163–1173. [PubMed: 29433850]
8. Abou-Alfa GK, Meyer T, Cheng AL, El-Khoueiry AB, Rimassa L, Ryoo BY, Cicin I, et al. Cabozantinib in Patients with Advanced and Progressing Hepatocellular Carcinoma. *N Engl J Med* 2018;379:54–63. [PubMed: 29972759]
9. Llovet JM, Hernandez-Gea V. Hepatocellular carcinoma: reasons for phase III failure and novel perspectives on trial design. *Clin Cancer Res* 2014;20:2072–2079. [PubMed: 24589894]
10. Chen L, Han X. Anti-PD-1/PD-L1 therapy of human cancer: past, present, and future. *J Clin Invest* 2015;125:3384–3391. [PubMed: 26325035]
11. Whiteside TL, Demaria S, Rodriguez-Ruiz ME, Zarour HM, Melero I. Emerging Opportunities and Challenges in Cancer Immunotherapy. *Clin Cancer Res* 2016;22:1845–1855. [PubMed: 27084738]
12. Topalian SL, Drake CG, Pardoll DM. Immune checkpoint blockade: a common denominator approach to cancer therapy. *Cancer Cell* 2015;27:450–461. [PubMed: 25858804]
13. Makarova-Rusher OV, Medina-Echeverz J, Duffy AG, Greten TF. The yin and yang of evasion and immune activation in HCC. *J Hepatol* 2015;62:1420–1429. [PubMed: 25733155]
14. Hato T, Goyal L, Greten TF, Duda DG, Zhu AX. Immune checkpoint blockade in hepatocellular carcinoma: current progress and future directions. *Hepatology* 2014;60:1776–1782. [PubMed: 24912948]
15. El-Khoueiry AB, Sangro B, Yau T, Crocenzi TS, Kudo M, Hsu C, Kim TY, et al. Nivolumab in patients with advanced hepatocellular carcinoma (CheckMate 040): an open-label, non-comparative, phase 1/2 dose escalation and expansion trial. *Lancet* 2017;389:2492–2502. [PubMed: 28434648]
16. Zhu AX, Finn RS, Edeline J, Cattani S, Ogasawara S, Palmer D, Verslype C, et al. Pembrolizumab in patients with advanced hepatocellular carcinoma previously treated with sorafenib (KEYNOTE-224): a non-randomised, open-label phase 2 trial. *Lancet Oncol* 2018;19:940–952. [PubMed: 29875066]
17. Jenne CN, Kubes P. Immune surveillance by the liver. *Nat Immunol* 2013;14:996–1006. [PubMed: 24048121]
18. Gao B, Jeong WI, Tian Z. Liver: An organ with predominant innate immunity. *Hepatology* 2008;47:729–736. [PubMed: 18167066]
19. Greten TF, Sangro B. Targets for immunotherapy of liver cancer. *J Hepatol* 2017.
20. Lee J, Liao R, Wang G, Yang BH, Luo X, Varki NM, Qiu SJ, et al. Preventive Inhibition of Liver Tumorigenesis by Systemic Activation of Innate Immune Functions. *Cell Rep* 2017;21:1870–1882. [PubMed: 29141219]
21. Chen X, Calvisi DF. Hydrodynamic transfection for generation of novel mouse models for liver cancer research. *The American journal of pathology* 2014;184:912–923. [PubMed: 24480331]
22. Liu JJ, Li Y, Chen WS, Liang Y, Wang G, Zong M, Kaneko K, et al. Shp2 deletion in hepatocytes suppresses hepatocarcinogenesis driven by oncogenic beta-Catenin, PIK3CA and MET. *J Hepatol* 2018;69:79–88. [PubMed: 29505847]
23. Liang Y, Feng Y, Zong M, Wei XF, Lee J, Feng Y, Li H, et al. beta-catenin deficiency in hepatocytes aggravates hepatocarcinogenesis driven by oncogenic beta-catenin and MET. *Hepatology* 2018;67:1807–1822. [PubMed: 29152756]
24. Heinecke L, Proud D, Sanders S, Schleimer RP, Kim J. Induction of B7-H1 and B7-DC expression on airway epithelial cells by the Toll-like receptor 3 agonist double-stranded RNA and human rhinovirus infection: In vivo and in vitro studies. *J Allergy Clin Immunol* 2008;121:1155–1160. [PubMed: 18378285]
25. Telcian AG, Laza-Stanca V, Edwards MR, Harker JA, Wang H, Bartlett NW, Mallia P, et al. RSV-induced bronchial epithelial cell PD-L1 expression inhibits CD8+ T cell nonspecific antiviral activity. *J Infect Dis* 2011;203:85–94. [PubMed: 21148500]
26. Salmon H, Idoyaga J, Rahman A, Leboeuf M, Remark R, Jordan S, Casanova-Acebes M, et al. Expansion and Activation of CD103(+) Dendritic Cell Progenitors at the Tumor Site Enhances

- Tumor Responses to Therapeutic PD-L1 and BRAF Inhibition. *Immunity* 2016;44:924–938. [PubMed: 27096321]
27. Hong S, Chen N, Fang W, Zhan J, Liu Q, Kang S, He X, et al. Upregulation of PD-L1 by EML4-ALK fusion protein mediates the immune escape in ALK positive NSCLC: Implication for optional anti-PD-1/PD-L1 immune therapy for ALK-TKIs sensitive and resistant NSCLC patients. *Oncoimmunology* 2016;5:e1094598. [PubMed: 27141355]
  28. Shang N, Arteaga M, Zaidi A, Stauffer J, Cotler SJ, Zeleznik-Le NJ, Zhang J, et al. FAK is required for c-Met/beta-catenin-driven hepatocarcinogenesis. *Hepatology* 2015;61:214–226. [PubMed: 25163657]
  29. Zucman-Rossi J, Villanueva A, Nault JC, Llovet JM. Genetic Landscape and Biomarkers of Hepatocellular Carcinoma. *Gastroenterology* 2015;149:1226–1239 e1224. [PubMed: 26099527]
  30. Dunn GP, Koebel CM, Schreiber RD. Interferons, immunity and cancer immunoediting. *Nat Rev Immunol* 2006;6:836–848. [PubMed: 17063185]
  31. Ammi R, De Waele J, Willems Y, Van Brussel I, Schrijvers DM, Lion E, Smits EL. Poly(I:C) as cancer vaccine adjuvant: knocking on the door of medical breakthroughs. *Pharmacol Ther* 2015;146:120–131. [PubMed: 25281915]
  32. Datta SK, Redecke V, Prilliman KR, Takabayashi K, Corr M, Tallant T, DiDonato J, et al. A subset of Toll-like receptor ligands induces cross-presentation by bone marrow-derived dendritic cells. *J Immunol* 2003;170:4102–4110. [PubMed: 12682240]
  33. Schulz O, Diebold SS, Chen M, Naslund TI, Nolte MA, Alexopoulou L, Azuma YT, et al. Toll-like receptor 3 promotes cross-priming to virus-infected cells. *Nature* 2005;433:887–892. [PubMed: 15711573]
  34. McCartney S, Vermi W, Gilfillan S, Cella M, Murphy TL, Schreiber RD, Murphy KM, et al. Distinct and complementary functions of MDA5 and TLR3 in poly(I:C)-mediated activation of mouse NK cells. *J Exp Med* 2009;206:2967–2976. [PubMed: 19995959]
  35. Sivori S, Falco M, Della Chiesa M, Carlomagno S, Vitale M, Moretta L, Moretta A. CpG and double-stranded RNA trigger human NK cells by Toll-like receptors: induction of cytokine release and cytotoxicity against tumors and dendritic cells. *Proc Natl Acad Sci U S A* 2004;101:10116–10121. [PubMed: 15218108]
  36. Cheever MA. Twelve immunotherapy drugs that could cure cancers. *Immunol Rev* 2008;222:357–368. [PubMed: 18364014]
  37. Limmer A, Ohl J, Kurts C, Ljunggren HG, Reiss Y, Groettrup M, Momburg F, et al. Efficient presentation of exogenous antigen by liver endothelial cells to CD8+ T cells results in antigen-specific T-cell tolerance. *Nat Med* 2000;6:1348–1354. [PubMed: 11100119]
  38. Hochst B, Schildberg FA, Bottcher J, Metzger C, Huss S, Turler A, Overhaus M, et al. Liver sinusoidal endothelial cells contribute to CD8 T cell tolerance toward circulating carcinoembryonic antigen in mice. *Hepatology* 2012;56:1924–1933. [PubMed: 22610745]
  39. Nagato T, Lee YR, Harabuchi Y, Celis E. Combinatorial immunotherapy of polyinosinic-polycytidylic acid and blockade of programmed death-ligand 1 induce effective CD8 T-cell responses against established tumors. *Clin Cancer Res* 2014;20:1223–1234. [PubMed: 24389326]



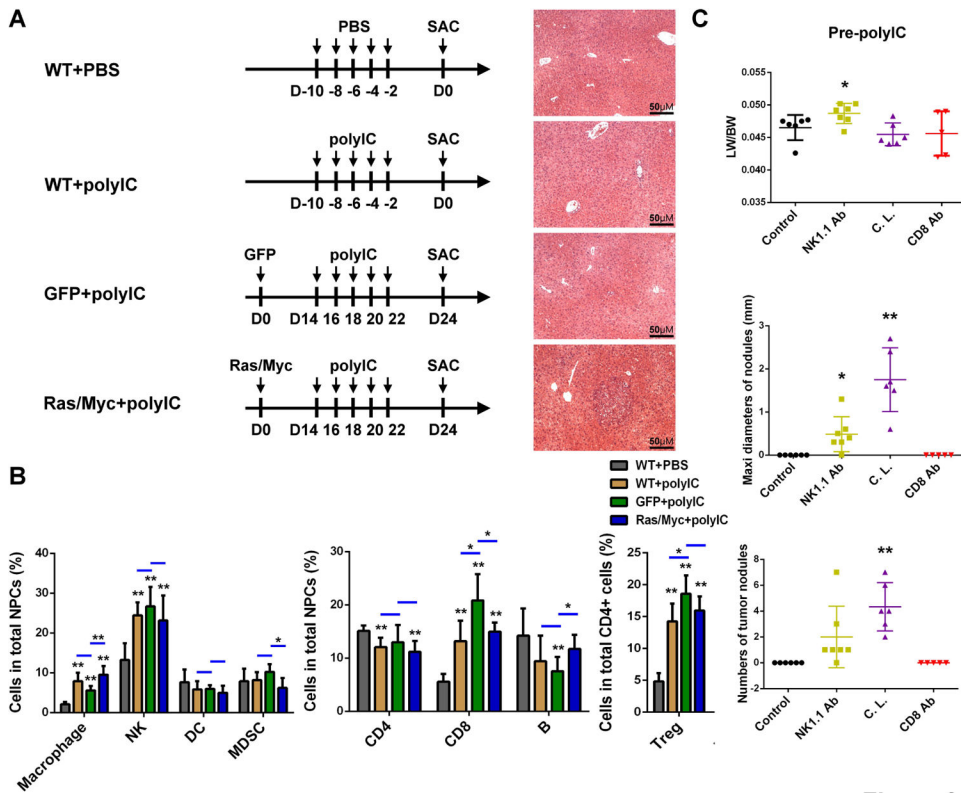


**Figure 2. The roles of innate immune cells in mediating polyIC inhibition of tumor initiation.**

(A) The scheme of experimental procedure. Mice were divided into four groups. In the first two groups (WT+PBS; WT+polyIC), WT mice were injected i.p. with PBS or polyIC (4  $\mu$ g/g of body weight), at -10, -8, -6, -4, -2 days before sacrifice (SAC) for analysis. The other two groups (GFP+polyIC; Ras/Myc+polyIC) of mice were injected with GFP or N-Ras/c-Myc plasmids at day 0, and were then i.p. injected with polyIC (4  $\mu$ g/g) at day 14, 16, 18, 20 and 22, before sacrifice (SAC) at day 24. The representative H&E stained liver sections are shown for each group. Magnification: x20; Scale bar: 50  $\mu$ m.

(B) Flow cytometry analysis was performed and the relative cell numbers of innate and adaptive immune cell subsets were quantified in the livers. Data are presented as means  $\pm$  SD (n=6 per group). \*p<0.05, \*\*p<0.01 for any other groups versus WT+PBS group, or as indicated by the horizontal line.

(C) Tumor burdens were calculated by LW/BW ratios, maximal diameters (mm) and numbers of tumor nodules, to evaluate the effects of depleting NK cells (NK1.1 Ab), macrophages (clondronate liposome, C.L.) or CD8 T cells (CD8 Ab) on polyIC inhibition of HCC initiation. Data are presented as means  $\pm$  SD (n=5-7 per group). \*p<0.05, \*\*p<0.01 for any other groups versus control.

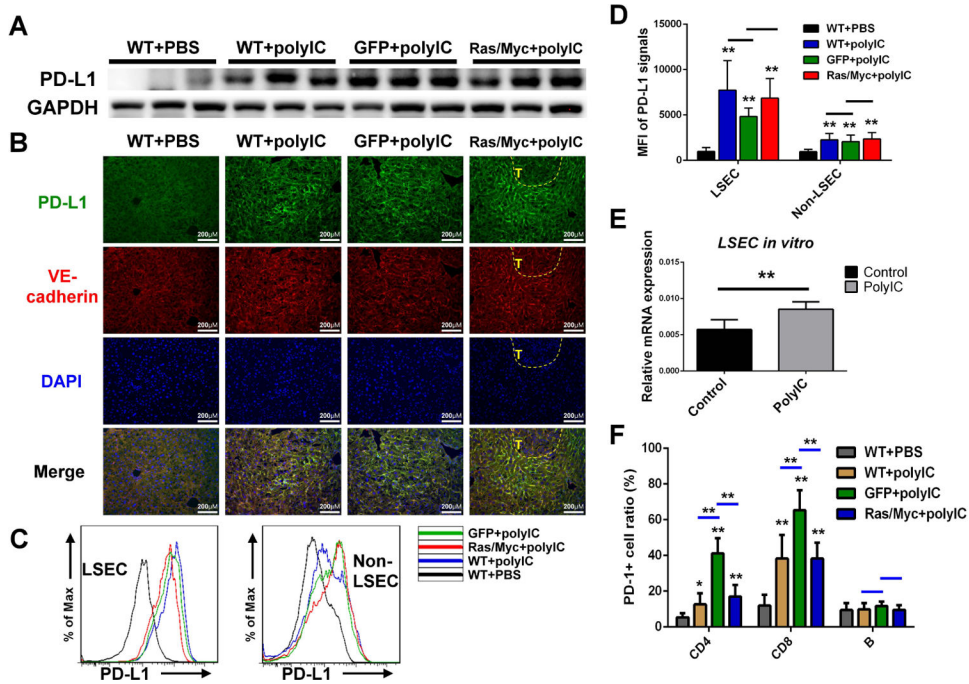


**Figure 3. polyIC upregulates PD-L1 expression in LSECs.**

(A) Immunoblot analysis of PD-L1 expression in liver lysates of four groups (n=3 per group), as in figure 2A with GAPDH as loading control.

(B) Representative immunostaining of PD-L1 (green) and VE-cadherin (red) in liver sections, magnification: x40; scale bar: 25  $\mu$ m.

(C) Flow cytometry analysis to show the representative PD-L1 expression in LSECs and other NPCs (non-LSECs) in four groups of livers (n=6 per group) as indicated.

(D) Quantification of mean fluorescence intensity (MFI) of PD-L1 expression in LSECs and non-LSECs in four groups of livers.

(E) Relative mRNA levels of PD-L1 expression in isolated LSECs after treatment with PBS or polyIC (80  $\mu$ g/mL) for 2 days in vitro.

(F) Flow cytometry analysis and quantification for the ratios of PD-1<sup>+</sup> cells in CD4, CD8 T cells and B cells in livers as indicated. Data in (D, F) are presented as means  $\pm$  SD (n=6 per group) for any other groups versus WT+PBS, or indicated by a horizontal line. Data in (E) are presented as means  $\pm$  SD (n=4 per group). \*p<0.05, \*\*p<0.01.

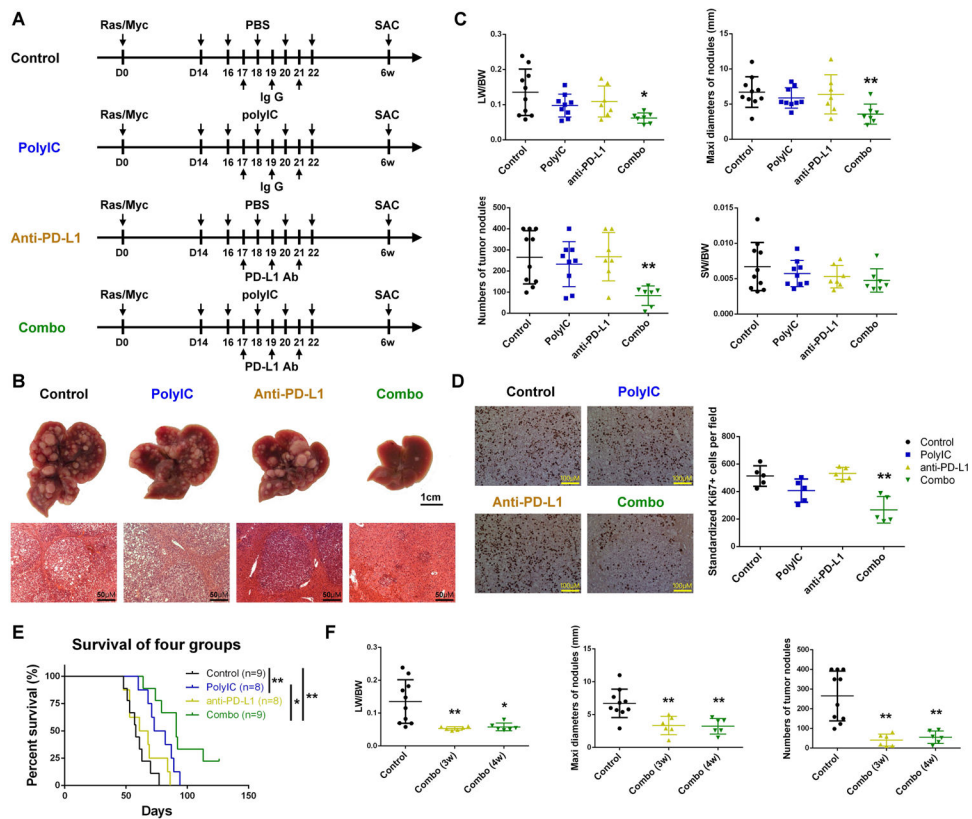


**Figure 4. polyIC sensitizes PD-L1 blockade in HCC treatment in mice.**

(A) The scheme of experimental procedure for polyIC, PD-L1 Ab or their combination treatment (Combo). N-Ras/c-Myc were transfected into all four groups of mice at day 0. polyIC (4  $\mu$ g/g) (or PBS) was i.p. injected at day 14, 16, 18, 20 and 22, and PD-L1 Ab (or isotype IgG) was i.p. injected at day 17, 19 and 21. All mice were sacrificed (SAC) 6 weeks after oncogene transfection.

(B) Representative macroscopic views and H&E stained liver sections in mice of control, polyIC, anti-PD-L1 and Combo treatment. Magnification: x20; Scale bar: 50  $\mu$ m.

(C) Tumor loads were evaluated by LW/BW ratios, maximal diameters (mm) and numbers of nodules, with the ratios of spleen weight/body weight (SW/BW) also measured.

(D) Left: representative immunostaining of Ki67 in tumor areas in liver sections. Magnification: x40; Scale bar: 25  $\mu$ m. Right: quantification of Ki67<sup>+</sup> tumor cell numbers per field.

(E) Kaplan-Meier survival curves of overall survival of the four groups of mice. A mouse was euthanized when it was found to be feeble and dilatory because of big tumor burden, and the death date was recorded as the next day. Log-rank test was performed, n=8–9 per group.

(F) The combined treatment started at 3 or 4 weeks after oncogene transfection, Combo (3w) and Combo (4w), and the control mice were transfected with Ras/Myc without receiving the treatment. Tumor burdens were measured 6 weeks after Ras/Myc transfection.



Data in (C, D, F) are presented as means  $\pm$  SD (n=7–9, n=5, n=6–10, respectively, per group). \*p<0.05, \*\*p<0.01, for any other groups versus control, or as indicated by vertical line in (E).

Author Manuscript

Author Manuscript

Author Manuscript

Author Manuscript

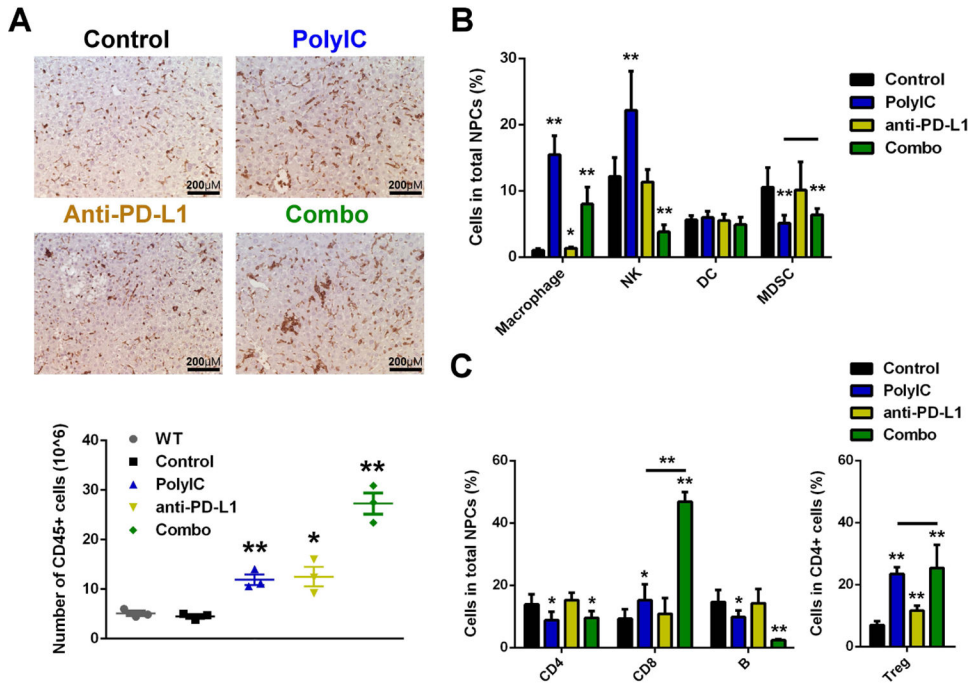


**Figure 5. Combined treatment of polyIC and PD-L1 Ab boosts innate and adaptive immunity in the liver.**

(A) Mice were transfected with Ras/Myc at day 0. polyIC (4 μg/g) or PBS was i.p. injected at day 14, 16, 18, 20 and 22, and PD-L1 Ab (or isotype IgG) was i.p. injected at day 17, 19 and 21. All mice were sacrificed (SAC) at day 24 for analysis. Top: representative immunostaining of CD45 in liver sections. Magnification: x40; Scale bar: 25 μm. Bottom: quantification of CD45<sup>+</sup> cell numbers isolated by MACS per mouse, with the WT group indicating mice without any treatment.

(B) Flow cytometry analysis was performed and quantified for the relative ratios of macrophages, NK, DC and MDSC in the total NPCs.

(C) Flow cytometry analysis was performed and quantified for the relative ratios of CD4, CD8 T cells and B cells in the total NPCs, and Treg in the CD4 T cells.

Data are presented as mean ± SD (A: n=3 per group; B, C: n=6 per group). \*p<0.05, \*\*p<0.01, for any other group versus control, or as indicated by horizontal line in (B, C).

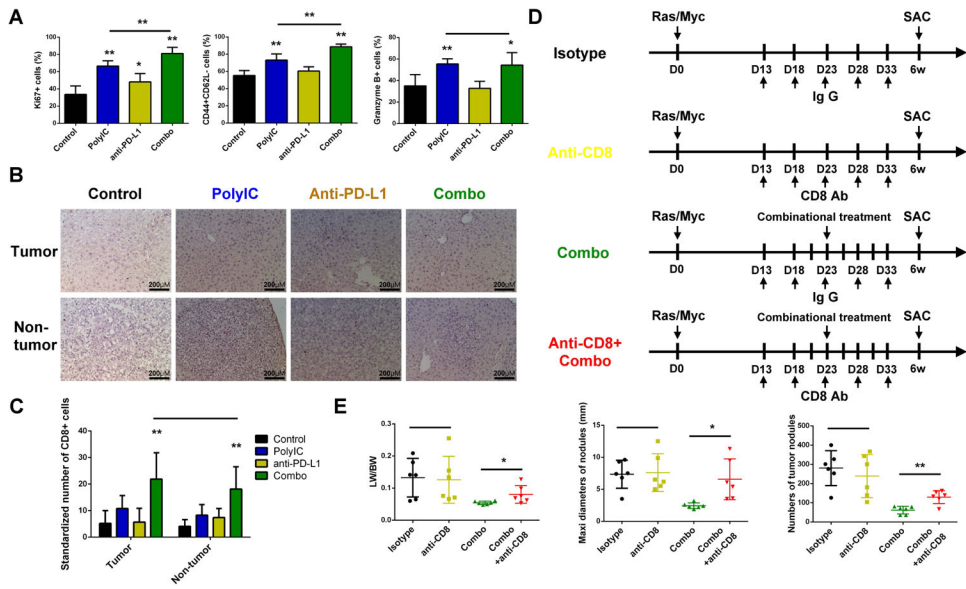


**Figure 6. The enhanced anti-tumor effect of polyIC and PD-L1 blockade is cytotoxic T cell dependent.**

(A) Flow cytometry analysis was performed to determine the ratios of cytotoxic T cell proliferation (Ki67<sup>+</sup>), activation (CD44<sup>+</sup>CD62L<sup>-</sup>) and cytotoxic function (granzyme B<sup>+</sup>) in total CD8 T cells, in livers of four groups, as shown in figure 5A.

(B) Representative immunostaining of CD8 in tumor and non-tumor areas in liver sections, as shown in figure 4A. Magnification: x40; Scale bar: 25  $\mu$ m.

(C) Quantification of CD8<sup>+</sup> cell numbers per field in the tumor and non-tumor areas, respectively, in the liver sections, related to panel B.

(D) The scheme of experimental procedure for CD8 blockade. Ras/Myc were transfected into all mice at day 0. For the combination treatment, mice received polyIC (4  $\mu$ g/g) at day 14, 16, 18, 20, 22, and PD-L1 Ab (200  $\mu$ g) at day 17, 19 and 21. For CD8 blockade, CD8 Ab (200  $\mu$ g) (or isotype IgG, 200  $\mu$ g) was i.p. injected at day 13, 18, 23, 28 and 33. All mice were sacrificed (SAC) 6 weeks after oncogene transfection.

(E) Tumor burdens were evaluated as indicated, related to panel D.

Data in (A, C, E) are presented as means  $\pm$  SD (n=6, n=5-7, n=6, respectively, per group).

\*p<0.05, \*\*p<0.01, for any other group versus control, or indicated by horizontal line.

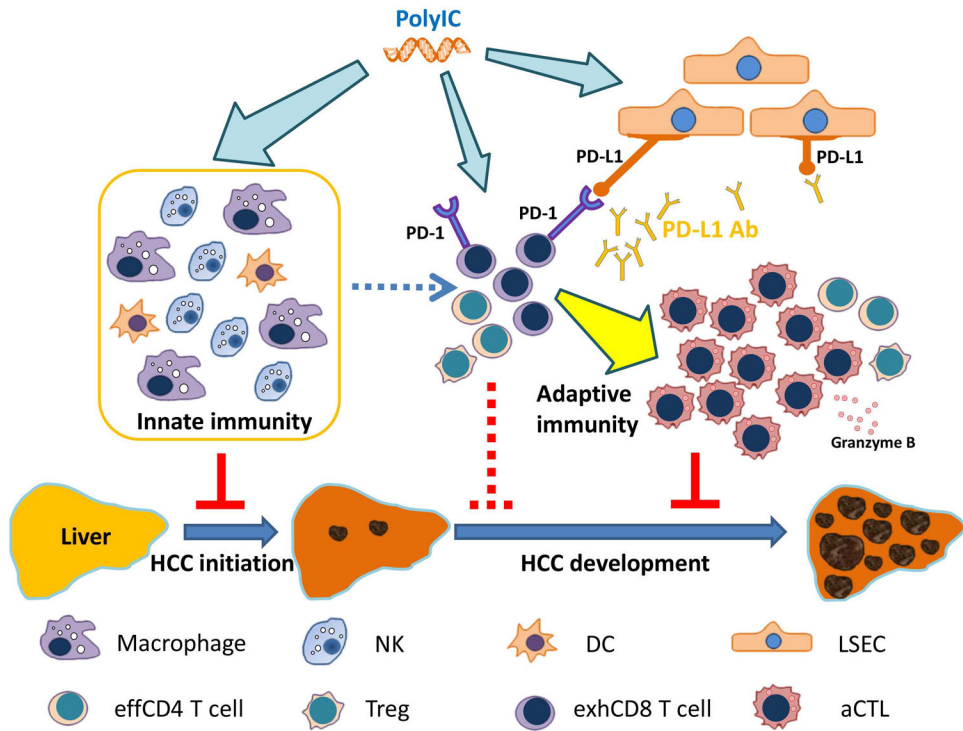


**Figure 7. A model for the tumor-suppressing effects of polyIC and/or PD-L1 blockade.** Injection of polyIC suppresses tumor initiation by activation of multiple innate immune cell functions, and its induction of PD-L1 expression in LSECs sensitizes liver response to anti-PD-L1 blockade. Thus, a combined treatment of polyIC and PD-L1 Ab may be an effective combination immunotherapy for liver cancer.  
 NK: Natural killer cell; DC: dendritic cell; LSEC: liver sinusoidal endothelial cell; effCD4 cell: effective CD4 T cell; Treg: regulatory T cell; exhCD8 T cell: exhausted CD8 T cell; aCTL: activated cytotoxic T cell.